

# JOURNAL OF SOLID STATE CHEMISTRY

Editor

**M.G. KANATZIDIS**

Associate Editors

**S.J. HWANG**

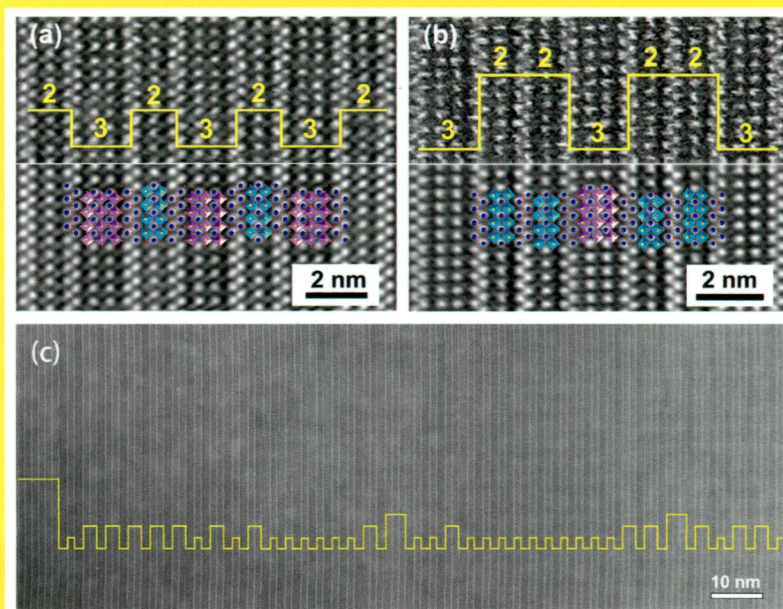
**J. LI**

**S.J. CLARKE**

**H.-C. ZUR LOYE**

IN THIS ISSUE:

**Local orderings in long-range-disordered bismuth-layered  
intergrowth structure**



**Faqlang Zhang, Yongxiang Li, Hui Gu and Xiang Gao**

Available online at [www.sciencedirect.com](http://www.sciencedirect.com)

**ScienceDirect**

J  
S  
S  
C

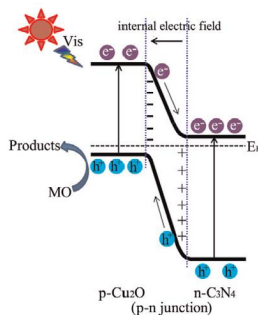


Abstracted/indexed in BioEngineering Abstracts, Chemical Abstracts, Coal Abstracts, Current Contents/Physics, Chemical, & Earth Sciences, Engineering Index, Research Alert, SCISEARCH, Science Abstracts, and Science Citation Index. Also covered in the abstract and citation database SCOPUS®. Full text available on ScienceDirect®.

## Regular Articles

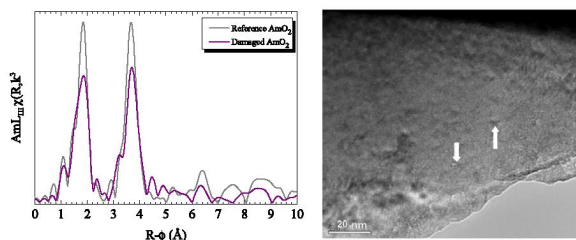
### Graphitic carbon nitride/Cu<sub>2</sub>O heterojunctions: Preparation, characterization, and enhanced photocatalytic activity under visible light

Yanlong Tian, Binbin Chang, Jie Fu, Baocheng Zhou, Jiyang Liu, Fengna Xi and Xiaoping Dong  
page 1



### Structural investigation of self-irradiation damaged AmO<sub>2</sub>

Damien Prieur, Jean-François Vigier, Thierry Wiss, Arne Janssen, Jörg Rothe, Andrea Cambriani and Joseph Somers  
page 7

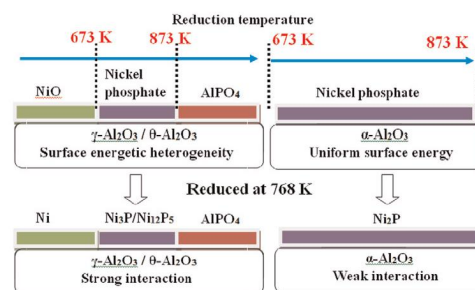


The structure of damaged AmO<sub>2</sub> (36 dpa) has been studied by XRD, XAS and TEM. Thus, the effects of the self-irradiation on the oxidation state, the lattice distances, the structural disorder, the radiation stability and the microstructure have been discussed.

## Regular Articles—Continued

### Essential elucidation for preparation of supported nickel phosphide upon nickel phosphate precursor

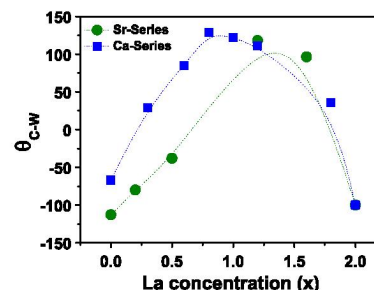
Xuguang Liu, Lei Xu and Baoquan Zhang  
page 13



Surface energy heterogeneity in alumina (namely  $\alpha$ -Al<sub>2</sub>O<sub>3</sub>,  $\theta$ -Al<sub>2</sub>O<sub>3</sub>, and  $\gamma$ -Al<sub>2</sub>O<sub>3</sub>) supported multi-oxidic precursors with different reducibilities and thus diverse nickel phosphides (*i.e.*, Ni<sub>3</sub>P, Ni<sub>12</sub>P<sub>5</sub>, Ni<sub>2</sub>P).

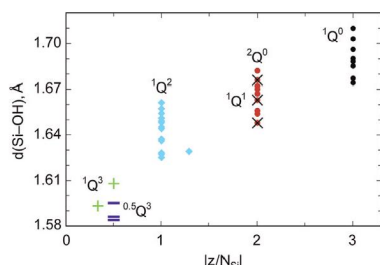
### Structural, electronic and magnetic properties of the series of double perovskites (Ca,Sr)<sub>2-x</sub>La<sub>x</sub>FeIrO<sub>6</sub>

L. Bufaical, C. Adriano, R. Lora-Serrano, J.G.S. Duque, L. Mendonça-Ferreira, C. Rojas-Ayala, E. Baggio-Saitovitch, E.M. Bittar and P.G. Pagliuso  
page 23



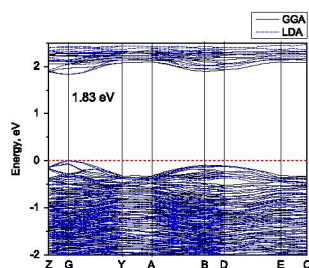
The Weiss constant as a function of La doping for the (Ca,Sr)<sub>2-x</sub>La<sub>x</sub>FeIrO<sub>6</sub> series, indicating changes in Fe–Ir magnetic coupling on both families.

**Compositional effects on Si–OH bond length in hydrous silicates with implications for trends in the SiOH acidity**  
Dmitri P. Zarubin  
page 30



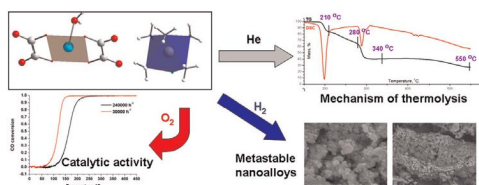
Si–OH bonds in crystalline silicates lengthen with the anionic charge per tetrahedron, which is in parallel with the well-known trend of decreased acidity of silicic acids and silicas in solution with increased degree of deprotonation.

**First-principles studies of the structural, electronic, and optical properties of a novel thorium compound  $\text{Rb}_2\text{Th}_7\text{Se}_{15}$**   
M.G. Brik  
page 37

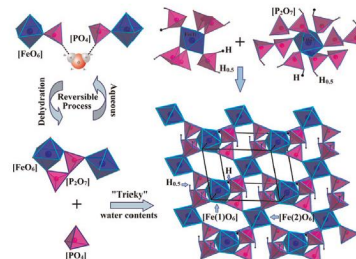


Calculated band structure of  $\text{Rb}_2\text{Th}_7\text{Se}_{15}$ .

**Low temperature synthesis of Ru–Cu alloy nanoparticles with the compositions in the miscibility gap**  
S.A. Martynova, E.Yu. Filatov, S.V. Korenev, N.V. Kuratieva, L.A. Sheludyakova, P.E. Plusnin, Yu.V. Shubin, E.M. Slavinskaya and A.I. Boronin  
page 42

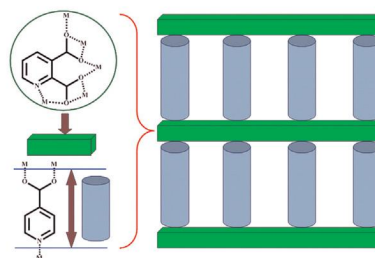


**Synthesis and characterization of novel barium iron phosphates: Insight into new structure types tailored by hydrogen atoms**  
Li-Zhi Sun, Wei Sun, Wei-Jian Ren, Jia-Ying Zhang, Ya-Xi Huang, Zhi-Mei Sun, Yuanming Pan and Jin-Xiao Mi  
page 48



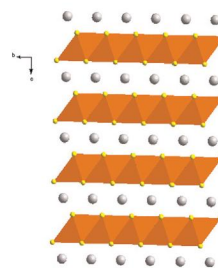
A new route of controlled water activities led to syntheses of three new compounds, indicating water plays a crucial role in the formation of novel phosphates.

**Luminescent pillared  $\text{Ln}^{\text{III}}$ – $\text{Zn}^{\text{II}}$  heterometallic coordination frameworks with two kinds of *N*-heterocyclic carboxylate ligands**  
Sui-Jun Liu, Ji-Min Jia, Yu Cui, Song-De Han and Ze Chang  
page 58



Four new 3D  $\text{Ln}^{\text{III}}$ – $\text{Zn}^{\text{II}}$  coordination frameworks with “pillar-layer” *sit* or *pcu* alpha-Po topology have been successfully obtained. Moreover, the photoluminescent properties of compounds **1–4** have also been investigated.

**Synthesis and high temperature transport properties of new quaternary layered selenide  $\text{NaCuMnSe}_2$**   
V. Pavan Kumar and U.V. Varadaraju  
page 64

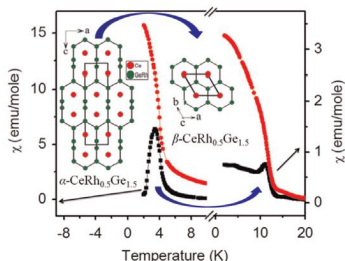


Crystal structure of  $\text{NaCuMnSe}_2$ .

## Structural and magnetic properties in the polymorphs of $\text{CeRh}_{0.5}\text{Ge}_{1.5}$

Deepti Kalsi, Udumula Subbarao, Sudhindra Rayaprol and Sebastian C. Peter

page 73

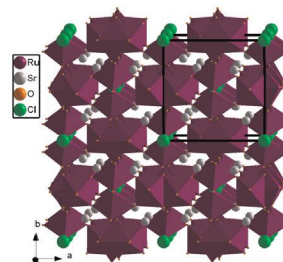


Two polymorphs of a new compound  $\text{CeRh}_{0.5}\text{Ge}_{1.5}$  in the  $\alpha\text{-ThSi}_2$  and  $\text{AlB}_2$  structure types were synthesized by arc melting. The magnetic measurements of both  $\text{CeRh}_{0.5}\text{Ge}_{1.5}$  phases suggest spin-glass behavior.

## $\text{Sr}_4\text{Ru}_6\text{ClO}_{18}$ , a new $\text{Ru}^{4+/5+}$ oxy-chloride, solved by precession electron diffraction: Electric and magnetic behavior

Pascal Roussel, Lukas Palatinus, Frédéric Belva, Sylvie Daviero-Minaud, Olivier Mentre and Marielle Huve

page 99

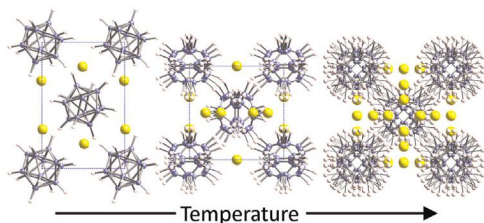


Structure of  $\text{Sr}_4\text{Ru}_6\text{ClO}_{18}$ , determined using Precession Electron Diffraction data.

## Complex high-temperature phase transitions in $\text{Li}_2\text{B}_{12}\text{H}_{12}$ and $\text{Na}_2\text{B}_{12}\text{H}_{12}$

Nina Verdal, Jae-Hyuk Her, Vitalie Stavila, Alexei V. Soloninin, Olga A. Babanova, Alexander V. Skripov, Terrence J. Udovic and John J. Rush

page 81

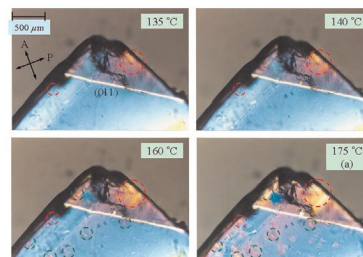


$\text{Na}_2\text{B}_{12}\text{H}_{12}$  undergoes a phase transformation from an ordered monoclinic structure at low temperature to a partially disordered body-centered-cubic (bcc) structure at  $\approx 529$  K, and finally to a more fully disordered bcc structure by  $\approx 545$  K.

## High-temperature phase transformation and topochemical nature in ferroelastic $(\text{NH}_4)_2\text{SO}_4$

Kwang-Sei Lee, In-Hwan Oh and Jae-Hyeon Ko

page 107

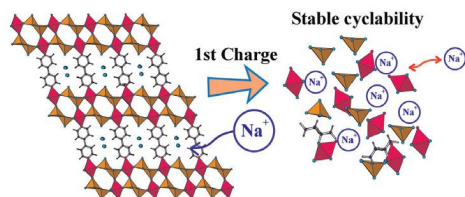


Surface morphology of the (100) face of  $(\text{NH}_4)_2\text{SO}_4$  on heating, showing chemical reaction at the surface.

## Electrochemical behavior of $[\{\text{Mn}(\text{Bpy})\}(\text{VO}_3)_2] \approx (\text{H}_2\text{O})_{1.24}$ and $[\{\text{Mn}(\text{Bpy})_{0.5}\}(\text{VO}_3)_2] \approx (\text{H}_2\text{O})_{0.62}$ inorganic-organic Brannerites in lithium and sodium cells

Roberto Fernández de Luis, Alexandre Ponrouch, M. Rosa Palacín, M. Karnele Urtiaga and María I. Arriortua

page 92

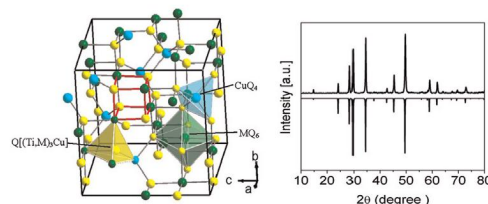


The electrochemical performance of  $[\{\text{Mn}(\text{Bpy})\}(\text{VO}_3)_2] \approx (\text{H}_2\text{O})_{1.16}$  and  $[\{\text{Mn}(\text{Bpy})_{0.5}\}(\text{VO}_3)_2] \approx (\text{H}_2\text{O})_{0.62}$  against sodium and lithium counter electrodes give rise to the structural collapse of the initial compounds. The IR and Raman studies show that the Bpy organic ligand is completely decomposed during the electrochemical testing. However, after the amorphization stable capacities as high as 850 mAh/g for lithium cells were achieved.

## Crystal structure and magnetic properties of titanium-based $\text{CuTi}_{2-x}\text{M}_x\text{S}_4$ and $\text{CuCr}_{2-x}\text{Ti}_x\text{Se}_4$ chalcospinels

P. Barahona, A. Galdámez, F. López-Vergara, V. Manríquez and O. Peña

page 114



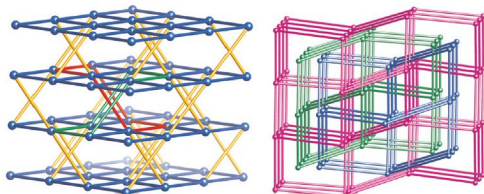
View along  $[100]$  of  $\text{CuCr}_{2-x}\text{Ti}_x\text{Se}_4$  crystal structure showing tetrahedral and octahedral units. To the right, experimental X-ray powder diffraction pattern of  $\text{CuCr}_{1.7}\text{Ti}_{0.3}\text{Se}_4$  (top) in compared (in a like-mirror representation) to a simulated X-ray pattern from single-crystal data (bottom).

Continued



**Cu<sup>II</sup> coordination polymers based on 5-methoxyisophthalate and flexible N-donor ligands: Structures and magnetic properties**

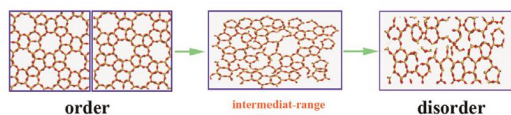
Xin-Hong Chang, Jian-Hua Qin, Lu-Fang Ma and Li-Ya Wang  
page 121



**Structures and magnetic properties of copper(II) coordination polymers constructed from 5-methoxyisophthalate linker and two flexible N-donor ancillary ligands.** Three copper(II) coordination polymers with 5-methoxyisophthalate and two related flexible N-donor ancillary ligands have been synthesized and structurally characterized. Moreover, thermal behaviors and magnetic properties of these complexes have also been investigated.

**The investigation of order–disorder transition process of ZSM-5 induced by spark plasma sintering**

Liang Wang, Lianjun Wang, Wan Jiang and He Lin  
page 128

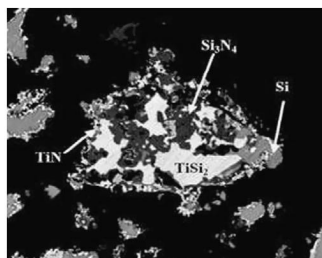


Note: The picture of ordered ZSM-5 comes from software material studio database

Low-density, ordered zeolites collapse to the rigid amorphous glass through spark plasma sintering. The intermediate-range structure formed in the process of order–disorder transition may give rise to specific property.

**Isothermal nitridation kinetics of TiSi<sub>2</sub> powders**

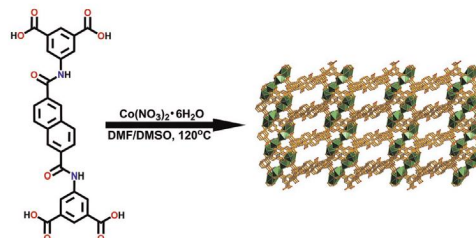
J. Roger, L. Maillé and M.A. Dourges  
page 134



Backscattered electrons image of a transverse TiSi<sub>2</sub> grain nitrated at 1100 °C for 50 h.

**A new 3D Co(II)–organic framework with acylamide-containing tetracarboxylate ligand: Solvothermal synthesis, crystal structure, gas adsorption and magnetic property**

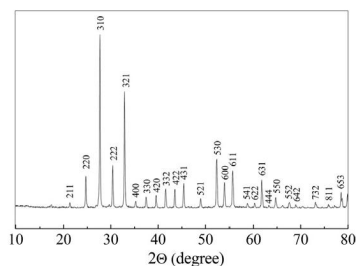
Qingfu Zhang, Haina Zhang, Aijing Geng, Suna Wang and Chong Zhang  
page 141



A new 3D Co(II)–organic framework with nanosized acylamide-containing tetracarboxylate ligand was solvothermally synthesized and structurally characterized, its thermal stability, gas adsorption and magnetic property were studied.

**Magnetization, magnetic susceptibility, effective magnetic moment of Fe<sup>3+</sup> ions in Bi<sub>25</sub>FeO<sub>39</sub> ferrite**

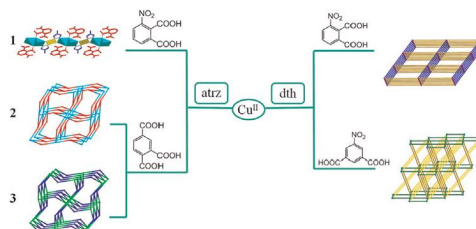
A.A. Zatsiupa, L.A. Bashkirov, I.O. Troyanchuk, G.S. Petrov, A.I. Galyas, L.S. Lobanovsky and S.V. Truhanov  
page 147



The dependence of the magnetization ( $n$ ,  $\mu_B$ ) on the magnetic field for one formula unit of Bi<sub>25</sub>FeO<sub>39</sub> at 5 K.

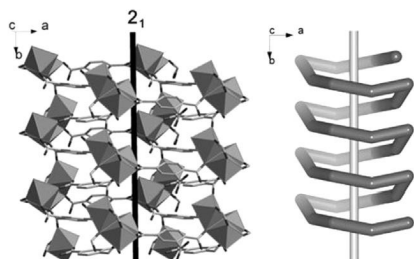
**Dimensional modulation and magnetic properties of triazole- and bis(triazole)-based copper(II) coordination polymers tuned by aromatic polycarboxylates**

Ju-Wen Zhang, Wei Zhao, Qi-Lin Lu, Jian Luan, Yun Qu and Xiu-Li Wang  
page 151



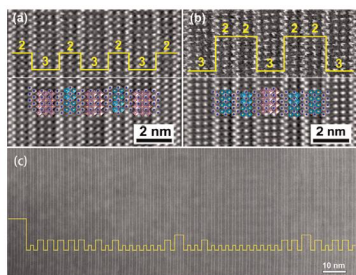
Five triazole-based copper(II) polymers modulated by polycarboxylates were synthesized. Bis-triazole-bis-amide ligand and polycarboxylates play important roles in tuning dimensionality of polymers. Magnetic properties of polymers were investigated.

**Studies of the structural and magnetic properties of an unsymmetrical ligand 1,2,4-benzenetricarboxylic acid based chiral 3-D trinickel coordination polymer as an alkali base-influenced hydrothermal reaction product**  
Yi-Ru Peng, Po-Hsiu Chien, Huey-Ting Chung, Pei-Yun Pan, Yen-Hsiang Liu and En-Che Yang  
*page 159*



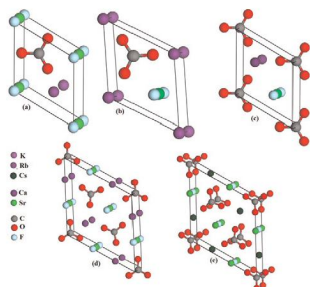
A chiral three-dimension MOF compound and its magnetic properties are described.

**Local orderings in long-range-disordered bismuth-layered intergrowth structure**  
Faqiang Zhang, Yongxiang Li, Hui Gu and Xiang Gao  
*page 165*



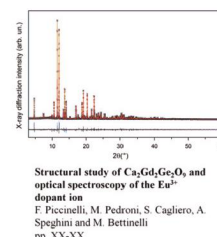
The long-range-disordered intergrowth structure in a  $(\text{Bi}_3\text{TiNbO}_9)_2$  ( $\text{Bi}_4\text{Ti}_3\text{O}_{12}$ ) ( $2 \times 2$ ) grain, which is composed of various types of local orderings, such as -22-, -23- and -223-.

**Structural, electronic and optical properties of novel carbonate fluorides  $\text{ABCO}_3\text{F}$  ( $\text{A}=\text{K}, \text{Rb}, \text{Cs}$ ;  $\text{B}=\text{Ca}, \text{Sr}$ )**  
E. Narsimha Rao, S. Appalakondaiah, N. Yedukondalu and G. Vaitheeswaran  
*page 171*



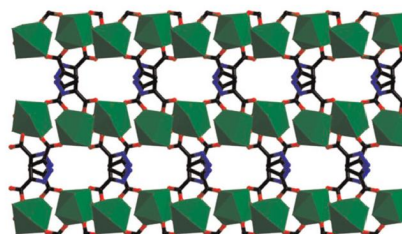
The co- and anti-parallel alignment of  $\text{CO}_3$  groups leads to larger and smaller SHG coefficients in (a)  $\text{KCaCO}_3\text{F}$ , (b)  $\text{KSrCO}_3\text{F}$ , (c)  $\text{RbCaCO}_3\text{F}$ , (d)  $\text{RbSrCO}_3\text{F}$ , and (e)  $\text{CsCaCO}_3\text{F}$ .

**Structural study of  $\text{Ca}_2\text{Gd}_2\text{Ge}_2\text{O}_9$  and optical spectroscopy of the  $\text{Eu}^{3+}$  dopant ion**  
Fabio Piccinelli, Marco Pedroni, Stefano Cagliero, Adolfo Speghini and Marco Bettinelli  
*page 180*



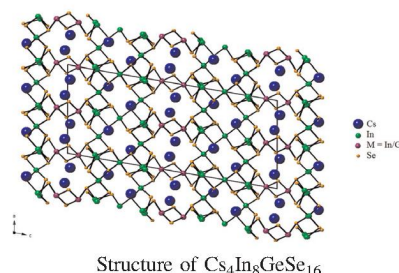
The structural study on  $\text{Ca}_2\text{Gd}_2\text{Ge}_2\text{O}_9$  exploiting synchrotron X-ray diffraction, allows us to determine the detailed geometry of the metal coordination polyhedra, which is closely related to the emission luminescence spectroscopy of the  $\text{Eu}^{3+}$  dopant ion introduced as impurity in this host.

**Syntheses, structures and properties of four 3D microporous lanthanide coordination polymers based on 3,5-pyrazoledicarboxylate and oxalate ligands**  
Juan Song, Ji-Jiang Wang, Huai-Ming Hu, Qing-Ran Wu, Juan Xie, Fa-Xin Dong, Meng-Lin Yang and Gang-Lin Xue  
*page 185*



Four 3D microporous lanthanide coordination polymers with reversible structural interconversion have been synthesized. They exhibit characteristic emission bands of the lanthanide ions and possess great thermal stability.

**Syntheses, structures, and optical properties of the indium/germanium selenides  $\text{Cs}_4\text{In}_8\text{GeSe}_{16}$ ,  $\text{CsInSe}_2$ , and  $\text{CsInGeSe}_4$**   
Matthew D. Ward, Eric A. Pozzi, Richard P. Van Duyne and James A. Ibers  
*page 191*



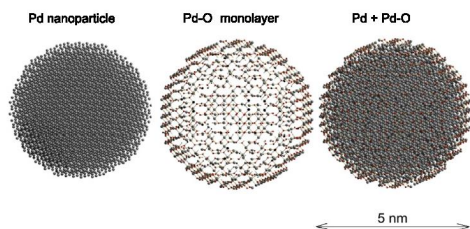
*Continued*



### The structure of nano-palladium deposited on carbon-based supports

Ľubomír Pikna, Ondrej Milkovič, Karel Saks, Mária Heželová, Miroslava Smrčová, Pavel Puliš, Štefan Michalik and Jana Gamcová

page 197

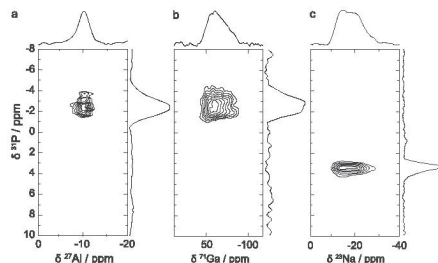


Visualization of metallic core (left), oxide monolayer (middle) and nanoparticle of diameter 5 nm (right).

### Cation substitution in $\beta$ -tricalcium phosphate investigated using multi-nuclear, solid-state NMR

Andrew T. Grigg, Martin Mee, Phillip M. Mallinson, Shirley K. Fong, Zhehong Gan, Ray Dupree and Diane Holland

page 227

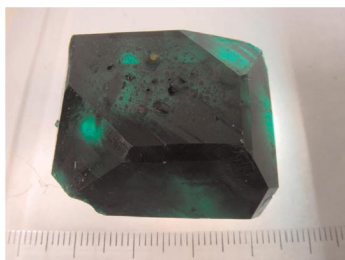


2D contour plots with skyline projections showing recoupling of  $^{27}\text{Al}$ ,  $^{71}\text{Ga}$  and  $^{23}\text{Na}$  to different  $^{31}\text{P}$  sites.

### Structure–property relations of orthorhombic $[(\text{CH}_3)_3\text{NCH}_2\text{COO}]_2(\text{CuCl}_2)_3 \cdot 2\text{H}_2\text{O}$

Eiken Haussühl, Jürgen Schreuer, Leonore Wiehl and Natalia Paulsen

page 205

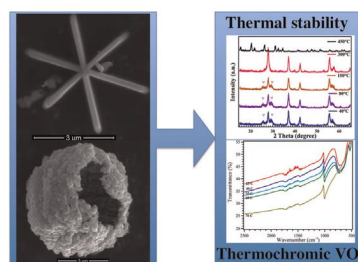


Single crystal of orthorhombic  $[(\text{CH}_3)_3\text{NCH}_2\text{COO}]_2(\text{CuCl}_2)_3 \cdot 2\text{H}_2\text{O}$ .

### Direct synthesis of thermochromic $\text{VO}_2$ through hydrothermal reaction

David Alie, Lynn Gedvilas, Zhiwei Wang, Robert Tenent, Chaiwat Engtrakul, Yanfa Yan, Sean E. Shaheen, Anne C. Dillon and Chunmei Ban

page 237

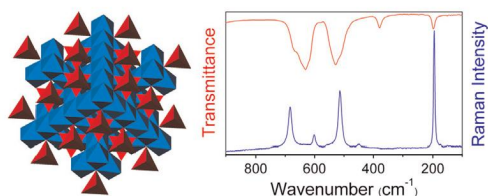


Thermochromic  $\text{VO}_2$  crystals with hollow spherical and asterisk shape were directly synthesized using hydrothermal techniques. X-ray diffraction (XRD) and Fourier transform infrared spectroscopy (FTIR) studies confirmed the thermal stability and the reversible thermochromic properties of the  $\text{VO}_2$  structure.

### Magnetic and low temperature phonon studies of $\text{CoCr}_2\text{O}_4$ powders doped with Fe(III) and Ni(II) ions

M. Ptak, M. Mączka, A. Pikul, P.E. Tomaszewski and J. Hanuza

page 218

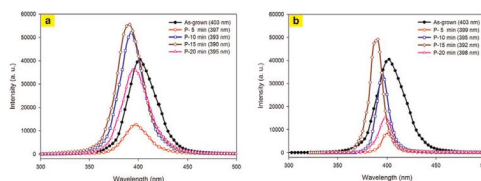


Visualization of normal spinel-type  $\text{AB}_2\text{O}_4$  structure, where blue octahedrons denote  $\text{BO}_6$  and red tetrahedrons  $\text{AO}_4$  units as well as IR and Raman spectra of  $\text{Co}_{0.9}\text{Ni}_{0.1}\text{Cr}_2\text{O}_4$  powder.

### Comparison of the structural and optical properties of porous $\text{In}_{0.08}\text{Ga}_{0.92}\text{N}$ thin films synthesized by electrochemical etching

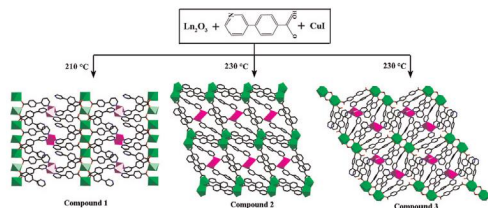
Saleh H. Abud, Z. Hassan, F.K. Yam and A.J. Ghazai

page 242



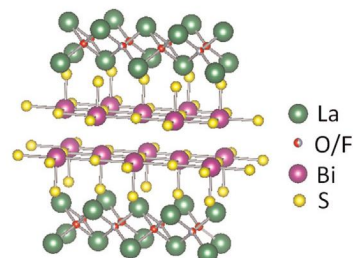
PL spectra of the as-grown and porous  $\text{In}_{0.08}\text{Ga}_{0.92}\text{N}$  under various etching duration.

**Syntheses and structures of three heterometallic coordination polymers derived from 4-pyridin-3-yl-benzoic acid**  
 Wei-Hui Fang and Guo-Yu Yang  
*page 249*



By hydrothermal reaction of lanthanide oxide, copper halide, and 4-pyridin-3-yl-benzoic ligand at different temperatures, a series of 1-D to 3-D 3d-4f coordination polymers, namely [ErL<sub>3</sub>(H<sub>2</sub>O)<sub>2</sub>][CuI], [Er<sub>2</sub>L<sub>6</sub>(H<sub>2</sub>O)][Cu<sub>2</sub>I<sub>2</sub>], [ErL<sub>3</sub>][CuI], and [Dy<sub>2</sub>L<sub>6</sub>(BPDC)<sub>0.5</sub>(H<sub>2</sub>O)<sub>4</sub>][Cu<sub>3</sub>I<sub>2</sub>], have been made, respectively.

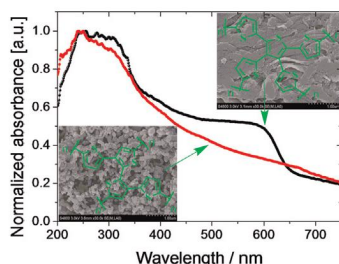
**Crystal structures of LaO<sub>1-x</sub>F<sub>x</sub>BiS<sub>2</sub> (x~0.23, 0.46): Effect of F doping on distortion of Bi-S plane**  
 Akira Miura, Masanori Nagao, Takahiro Takei, Satoshi Watauchi, Isao Tanaka and Nobuhiro Kumada  
*page 213*



Distortion of the Bi-S plane in LaO<sub>1-x</sub>F<sub>x</sub>BiS<sub>2</sub> changed when the F content was increased from 0.23 to 0.46, and a nearly flat Bi-S plane was formed at x~0.46 with the appearance of superconductivity.

**Rapid Communications**

**Influence of aggregated morphology on carbon dioxide uptake of polythiophene conjugated organic networks**  
 Shanlin Qiao, Zhengkun Du, Wei Huang and Renqiang Yang  
*page 69*



Two thiophene-based conjugated networks were prepared with different steric configuration building blocks, and they show various CO<sub>2</sub> uptake capacity and sorption isosteric enthalpies, although they have identical chemical constitution.

**Language services.** Authors who require information about language editing and copyediting services pre- and post-submission please visit <http://www.elsevier.com/locate/languagepolishing> or our customer support site at <http://epsupport.elsevier.com>. Please note Elsevier neither endorses nor takes responsibility for any products, goods or services offered by outside vendors through our services or in any advertising. For more information please refer to our Terms & Conditions <http://www.elsevier.com/termsandconditions>

For a full and complete Guide for Authors, please go to: <http://www.elsevier.com/locate/jssc>

*Journal of Solid State Chemistry* has no page charges.